PNAS

www.pnas.org

Coupling stabilizers open K$_V$1-type potassium channels

Malin Silverå Ejneby,[a] Björn Wallner,[b] Fredrik Elinder[a]*

[a]Department of Biomedical and Clinical Sciences, Linköping University, SE-581 85 Linköping, Sweden
[b]Department of Physics, Chemistry, and Biology, Linköping University, SE-581 83 Linköping, Sweden

*Corresponding Author
Fredrik Elinder
Department of Biomedical and Clinical Sciences, Linköping University, SE-581 85 Linköping, Sweden
Telephone: +46-732-707715
E-mail: fredrik.elinder@liu.se

This PDF file includes:

Detailed Materials and Methods
SI References
Figures S1-S9
Table S1

Supplementary Materials and Methods

Studied K$_V$ channels and Molecular biology. The *Drosophila* Shaker H4 channel (1) with removed N-type inactivation (ShH4IR) (2) in expression plasmid Bluescript II KS(+), is referred to as the wild-type (WT) Shaker K$_V$ channel. Point mutations were introduced using site-directed mutagenesis (QuikChange II, Aligent, CA, USA), and verified by sequencing at a core facility at Linköping University. cRNA (from linearized DNA) was prepared using the mMessage mMachine T7 kit (Invitrogen, CA, USA). To screen for channel-opening compounds (see below) we used a modified, so-called 3R Shaker K$_V$ channel, with two introduced positively charged arginines (M356R and A359R), in addition to one native arginine (R362), at the extracellular top of the voltage sensor. The 3R mutant is more sensitive to some channel-opening compounds that act via an electrostatic mechanism of action, such as polyunsaturated fatty acids (PUFAs) and resin acids (3). Therefore, we reasoned that this channel would increase our chances to find channel-opening compounds (acting via this mechanism). Human K$_V$1.5 (in pXOON), K$_V$2.1 (in pGem-HE), K$_V$4.1 (in pGem), K$_V$7.2, and K$_V$7.3, were also injected into *Xenopus leavis* oocytes for manual electrophysiological experiments. K$_V$7.2/7.3 was injected in a 1:1 ratio as described previously (4).

High-throughput screen: Cell culture and automated patch-clamp electrophysiology.
The details of the high-throughput screen have been described elsewhere ((5, 6) and references therein). In brief, the 3R Shaker K$_V$ channel was expressed in a CHO-K1 stable cell line. Recordings were performed using the PPC mode of the IonWorks Quattro automated patch-clamp system (Molecular Devices, Inc., Sunnyvale, CA, USA). The intracellular solution contained (in mM): 100 K-glutamate, 40 KCl, 3.2 MgCl$_2$, 3 EGTA and 5 HEPES (pH 7.25–7.3 with KOH) and the extracellular solution was D-PBS, (Gibco) and contained (in mM): 138 NaCl, 2.7 KCl, 1.5 KH$_2$PO$_4$, 8 Na$_2$HPO$_4$, 0.9 CaCl$_2$, 0.5 MgCl$_2$, and 5.5 glucose. To establish the whole-cell perforated patch configuration, amphotericin B was added to the intracellular solution. The holding voltage was –80 mV, and 150 ms voltage-clamp steps were applied to +10 mV, +30 mV, and +50 mV. The cells were kept at –80 mV for 300 ms between each step. The current signal was sampled at 10 kHz. All recordings were made at room temperature (~21°C).

High-throughput screen: Chemical libraries and compound handling. Compounds were searched for in the following chemical libraries; (Library name (Company or organization)): Acids (Vitas-M Laboratory Ltd); Consortium set (Specs)*; Drug Like (Enamine)*; Hit Finder (Maybridge)*; Ion Channel Ligand and Nuclear Receptor Ligand (Enzo Life Sciences Inc.); Known Drugs (Prestwick Chemical); LCBKI Primary Screening Set (Chemical Biology Consortium Sweden)*; Natural derivatives (TimTec); NIH Clinical Collection (National Institutes of Health); Peptidomimetics (ChemDiv Inc.)*; Tocriscreen Plus (Tocris Bioscience). Apart from LCBKI, provided by the Chemical Biology Consortium Sweden, and the NIH clinical collection, provided by the Libraries Roadmap Initiative, all compound libraries were commercially available. Whenever a selection was made (denoted by *), a chemist was instructed to search for small, hydrophobic, and partially charged compounds.

Assay-ready plates were prepared at the High Throughput Center at Karolinska Institutet. All compounds were dissolved in 100% dimethylsulfoxide (DMSO) to a final stock concentration of 10 mM. 100 nl of the 10 mM DMSO solutions of compounds and controls were transferred to low-volume 384-well polypropylene Greiner plates by acoustic dispensing (Echo 550,

Labcyte). The final concentration, in the test solution, was 10 µM of the compound. The tested compounds were added to the extracellular solution.

High-throughput screen: Analysis. Modulation of the K_V-mediated current was assessed by dividing the post-scan steady-state K_V current (for the last 10 ms of each pulse) by the respective pre-scan K_V current for each well. For the quantitative analysis presented in this paper, we used the data from +10 mV. In control solution (at +10 mV) during the experiment there was a consistent rundown of the current by $-20 \pm 7\%$ (mean ± SD). Therefore, all experimental data were adjusted for this rundown, were 1.00 means no effect. All data between 0.75 and 1.25 (mean ± 3 SD) were regarded as without effect (illustrated in Fig. 1B in the main text). If multiple experiments were carried out, we adjusted the significance level by dividing the deviation from 1 by $n^{0.5}$.

In total, we performed 16,230 recordings. 4130 of these were carried out with two compounds in each well to speed up the screen. If such a recording showed a significant effect, we retested both compounds separately. If not, these recordings were discarded from further analysis. Several of the most potent openers were tested in repeated recordings. Some compounds belonged to several chemical libraries, and were thus, unintentionally tested multiple times. Altogether, we obtained data from 10,096 unique compounds. Most of them were tested only in single experiments, but 1375 compounds were tested in duplicates, triplicates, or up to eight times. These multiple experiments allowed us to determine the inter-experimental root-mean-square deviation to 17%.

Frequency curves of the tautomer (and other) compounds among all 10,096 tested compounds versus effect on the current (Fig. 1D-E of the main text) were calculated as the weighted floated average value of data point in rank order with respect to both effect and frequency. In the x-axis range 0.46-1.50 all data points within ± 0.05 were included. The number of data for each point was 50-1700. Outside this range, the x-wise window was increased to make sure that 50 data were used for each average point. Above 3.60 the number of data decreased from 50 to 20. Thin lines represent a 95% confidence interval.

Calculated chemical properties. Marvin and JChem for Office (ChemAxon) were used for drawing chemical structures, calculate the molecular wight, the acidic dissociation constant (pK_a), and the octanol/water partitioning coefficient (log P) for uncharged compounds, as previously described (6, 7).

Calculation of side-chain effects. To get information about which side chains of the various tautomer compounds are important for channel opening, and to possibly get information about of the size and properties of the binding site, we performed a mathematical analysis based on a few assumptions. We assumed that the (1) side chains contribute to the channel-opening effect independently of each other, and (2) channel-opening effect depends on the product of the effect of the individual side chains. The first assumption is supported by the note that the central core is of general importance for channel opening. This suggests that the side chains, pointing in different directions could play independent roles. The second assumption is not very critical for the conclusions, but it should be noted that multiplication rather than addition gave a better fit to experimental data.

Among the 247 identified tautomer compounds there are 206 unique side chains, if a position dependence is taken into account. However, 15 molecules contain at least two unique side chains, which makes it impossible to determine the effect of these single side chains, and

these compounds are therefore left out from the analysis. 111 compounds have one unique side chain, which implies that by giving these side chains a specific value it will be possible to exactly predict the effect. The potential effect of these 111 unique side chains can be calculated post-analysis but these compounds cannot be used in the original analysis. The remaining 121 compounds have in total 68 unique side chains, and all share at least two distinct side chains with other compounds, which makes it meaningful to calculate the most likely effect of each side chain. To quantitatively analyze the role of the side chains we solved a system of 121 equations on the form

$$P_{R1x} * P_{R2x} * P_{R3x} * P_{R4x} = P_{totx}, \tag{1}$$

where P is the effect of each individual side chain (R1-R4) on channel opening for compound x, and P_{totx} is the total predicted effect of compound x. All equations must be coupled as all variables depend on each other. It is not possible to solve such a system in absolute terms but in relative terms. Therefore, we set the most prevalent side chains for R2 (benzyl group), R3 (methyl group) and R4 (hydrogen) to 1. This means that the absolute values cannot be compared between R1, R2, R3, and R4 but within each group. We then determined the best solution by a least-square method.

When all 68 variables were solved, these data were then used to calculate the effect of 111 other side chains (74 of them for R1) in 111 compounds. All side chain data are listed in Table S1. Despite the obvious risk of a transmitted error in the calculations, these calculated data were well in line with data for similar side chains in the original fit. This was a strong support for our performed analysis. Eight unique R1 side chains got values between 5 and 10, in parity with the most potent side chains from the fit. They all had one to two aromatic rings in different configurations.

All data from the screen is presented in Table. S1. Estimated effects for all side chains are also presented in this table. Selected data are presented in Fig. 2A in the main article. The side chains estimated to be most and least effective for respective position (R1-R4) are presented in Fig. 2B in the main article. Because only relative effects within a side chain family is of interest, we present the relative difference between the most and least effective side chains. If more than one side chain is presented, for the least or most effective side chains, we first calculated the (geometric) mean of the effects of these side chains, and then we calculated the relative difference between the most and least effective (clusters of) side chains.

Manual two-electrode voltage clamp recordings: Oocyte handling and two-electrode voltage-clamp recordings. All animal experiments were approved by Linköping's local Animal Care and Use Committee. Surgery of *Xenopus leavis* frogs, isolation of oocytes, and storage of oocytes, have been described in detail previously (5, 8). Oocytes were injected with RNA 1-6 days before two-electrode voltage-clamp (TEVC) experiments and stored at 8°C.

K^+ currents were measured with the TEVC technique (GeneClamp 500B amplifier, Axon instruments; Digidata 1440A converter, Molecular Devices; Clampex 10.5, Molecular Devices) as described previously (7). The holding voltage was generally set to -80 or -100 mV, and activation curves were usually generated in steps between -80 to $+50$ mV ($+5$ mV steps). Tail current for Kv7.2/7.3 was measured at -30 mV. The extracellular solution contained (in mM): 88 NaCl, 1 KCl, 0.8 $MgCl_2$, 0.4 $CaCl_2$ and 15 HEPES. pH was adjusted with NaOH. The test compounds, used for manual TEVC recordings, were initially dissolved in DMSO (to final stock concentration of 30 mM) and stored at -20 °C. The compound was

subsequently diluted in the extracellular solution to desired test concentration just prior to the experiment. The solution (with or without compound) was perfused to the recording chamber (0.5 ml/min) in a volume large enough to replace the existing solution in the chamber manifold. All experiments were done in room temperature. When testing the effect on different K_V channel a syringe was used to add the compound manually.

Manual two-electrode voltage clamp recordings: Analysis. The electrophysiological data were analysed using Clampfit 10.5 (Molecular Devices) and GraphPad Prism 8 (GraphPad software). The conductance, *G(V)*, was calculated as:

$$G(V) = I_K / (V - V_K) \qquad (2)$$

where I_K is the average steady-state current in the end of each activation step (WT and 3R Shaker K_V channel, $K_V1.5$ and $K_V2.1$), or the peak current for $K_V4.1$, V is the absolute membrane voltage, and V_K is the reversal potential (set to -80 mV). For the $K_V7.2/7.3$ channel the tail currents were measured 16 ms after onset at -30 mV, which then was plotted directly against the preceding test voltage to get a *G(V)* curve. The *G(V)* data was fitted to modified Boltzmann curve:

$$G(V) = A / (1 + \exp((V_{1/2} - V)/s))^n \qquad (3)$$

where *A* is the amplitude, $V_{1/2}$ is the midpoint (if $n = 1$), *s* is the slope, and *n* is an exponent (set to 4) for better curve fitting.

G(V) shifts were measured at the foot of the *G(V)* curve, at 10% of the maximal current amplitude in the control curve, or at 10% after the *G(V)* curves had been normalized (if the compound had a small additional blocking effect). This method has been described in detail before (9, 10). For $K_V2.1$ the currents were blocked, and the slope for the *G(V)* curve changed, so no accurate measurement of the *G(V)* shift could be made at the foot of the *G(V)* curve (Fig. S6E-F; Fig. 3E-F).

Concentration dependence, and pH dependence, for the compounds were quantified as:

$$\Delta V = V_{MAX} / (1 + c_{1/2} / c) \qquad (4)$$

where ΔV is the voltage shift, V_{MAX} is the amplitude, *c* is the concentration, and $c_{1/2}$ is the concentration at which half-maximum response occurs (or $pK_a = -\log(c_{1/2})$ for the pH dependence).

The time constant τ for opening and closing kinetics was calculated from a single exponential function

$$I(t) = A \exp(-t/\tau)) + C \qquad (5)$$

where *t* is the time, *A* is the amplitude, τ is the time constants, and *C* is a constant. The fit was performed by using Clampfit 10.7 (Levenberg-Marquardt search method; precision 10^{-6} with a maximum of 5000 iterations).

Molecular Docking. The 15 most potent compounds from the high-throughput screen (Table. S1) were docked against a model of all chains in the tetrameric Shaker K_V channel. The

model was constructed using HHpred (PMID:29258817) to find the most suitable template (2R9R) and Modeller (PMID:27322406) to build a homology model of chains. The initial model was minimized with constraints to starting position using Rosetta Relax application (PMID: 24265211), the lowest energy from ten independent relax runs was selected.

Compounds were converted from smiles to mol2 format using Open Babel 2.4.0 (PMID: 21982300), and conformers were generated using OpenEye Omega 3.1.1.2 (PMID: 20235588) with default settings. Charged versions of the compounds were constructed by deprotonate the polar hydrogens.

50,000 individual docking runs for each compound were performed using RosettaLigand (PMID:19041878). Each run was initialized by placing the compound randomly within a 5 Å sphere from any of the following amino acids: R377, K380, R387, and R487. Given that these amino acids are evenly positioned at the bottom of the channel, this sampling effectively places the compound anywhere at the bottom of the channel. A Monte Carlo procedure was used to minimize the energy by sampling the Cartesian and internal degrees of freedom of the compound using the conformer library, keeping the backbone of the channel fixed while allowing the side chains to adopt new conformations.

The docking runs were analyzed by counting how frequent the compound interacted with different amino acids in the 25 lowest docking poses, the exact number was not crucial and other thresholds gave similar results.

Statistical analysis. Mean values are expressed as mean ± SEM. A two-tailed one-sample t test, in which the mean value was compared with a hypothetical value of 0 was used to analyze $G(V)$ shifts. To compare two different conditions a Student's t-test was used. $p < 0.05$ was considered significant for all statistical tests. * $p < 0.05$, ** $p < 0.01$, *** $p < 0.001$.

References

1. A. Kamb, L. E. Iverson, M. A. Tanouye, Molecular characterization of Shaker, a Drosophila gene that encodes a potassium channel. *Cell* **50**, 405–413 (1987).

2. T. Hoshi, W. N. Zagotta, R. W. Aldrich, Biophysical and molecular mechanisms of Shaker potassium channel inactivation. *Science* **250**, 533–538 (1990).

3. N. E. Ottosson, S. I. Liin, F. Elinder, Drug-induced ion channel opening tuned by the voltage sensor charge profile. *J Gen Physiol* **143**, 173–182 (2014).

4. S. I. Liin, U. Karlsson, B. H. Bentzen, N. Schmitt, F. Elinder, Polyunsaturated fatty acids are potent openers of human M-channels expressed in Xenopus laevis oocytes. *Acta Physiol (Oxf)* **218**, 28–37 (2016).

5. N. E. Ottosson, *et al.*, Resin-acid derivatives as potent electrostatic openers of voltage-gated K channels and suppressors of neuronal excitability. *Sci Rep* **5**, 13278 (2015).

6. S. I. Liin, *et al.*, Biaryl sulfonamide motifs up- or down-regulate ion channel activity by activating voltage sensors. *J. Gen. Physiol.* **150**, 1215–1230 (2018).

7. M. Silverå Ejneby, *et al.*, Ahtom-by-atom tuning of the electrostatic potassium-channel modulator dehydroabietic acid. *J. Gen. Physiol.* **150**, 731–750 (2018).

8. S. I. Börjesson, T. Parkkari, S. Hammarström, F. Elinder, Electrostatic Tuning of Cellular Excitability. *Biophys J* **98**, 396–403 (2010).

9. S. I. Börjesson, S. Hammarström, F. Elinder, Lipoelectric modification of ion channel voltage gating by polyunsaturated fatty acids. *Biophys. J.* **95**, 2242–2253 (2008).

10. N. E. Ottosson, *et al.*, A drug pocket at the lipid bilayer-potassium channel interface. *Sci Adv* **3**, e1701099 (2017).

SI Figures
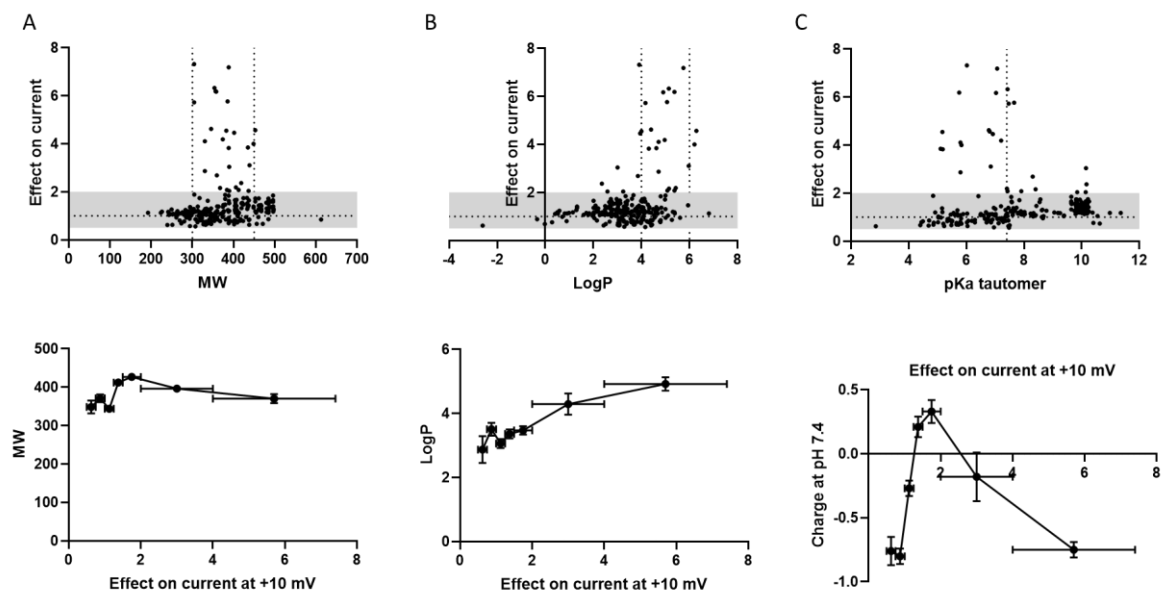
Fig. S1. **Chemical properties of the tautomer compounds versus their effect in the high-throughput screen.** (A) Molecular weights (MW) range from 200 to 500 for all but two of the compounds. All potent openers (>2, above the grey field) are within the range 300-450 (upper panel). There was no correlation between molecular weight and the effect (lower panel). (B) The most potent openers had LogP-values between 4 and 6 (upper panel). The LogP value increases for compounds with larger effects (lower panel). (C) The tautomer motif is expected to be partially negatively charged at neutral pH, and effectively the charge is then located to the carbon with the R1 chain (see Fig. 1C in main article). The best channel openers and all blockers have a pK_a value <7.4 (upper panel), so a negative charge of the tautomer motif is suggested to be important for gating effects even though some weak openers seem to have an uncharged tautomer motif. The calculated total charge of the molecule (not only the tautomer motif) at pH 7.4 depends on the effect of the molecule. Blockers and the best openers have a charge of almost −1, while compounds with no effect or with a small opening effect have a charge close to 0 (lower panel).
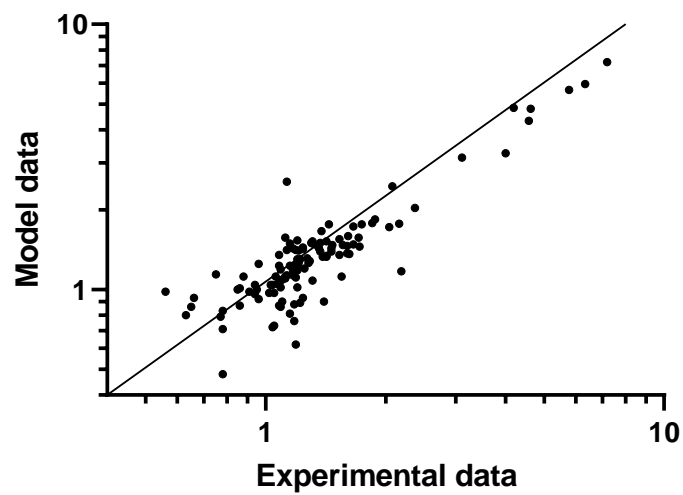
Fig. S2. The total predicted effect after side-chain calculations (Model data, Table S1) for the compounds used in the original analysis, plotted against the experimental data from the hight-throughput screen. Most compounds are close to the 1:1 line.
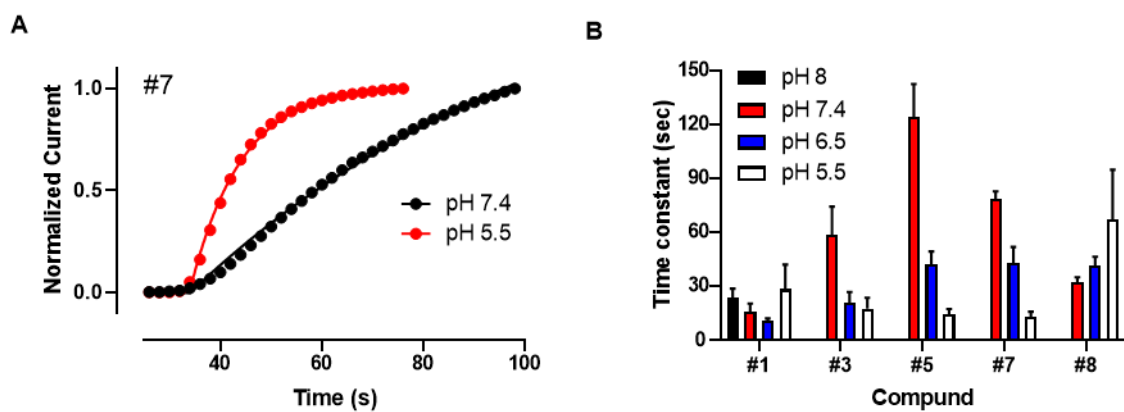
Fig. S3. Effects of pH on the onset of the effect. (A) The onset of the effect is faster at low pH. (B) Time constants of onset for five compounds at different pHs. For compounds #1 and #8 and pH 5.5 the solubility is decreased, possibly explaining the increased time constants.
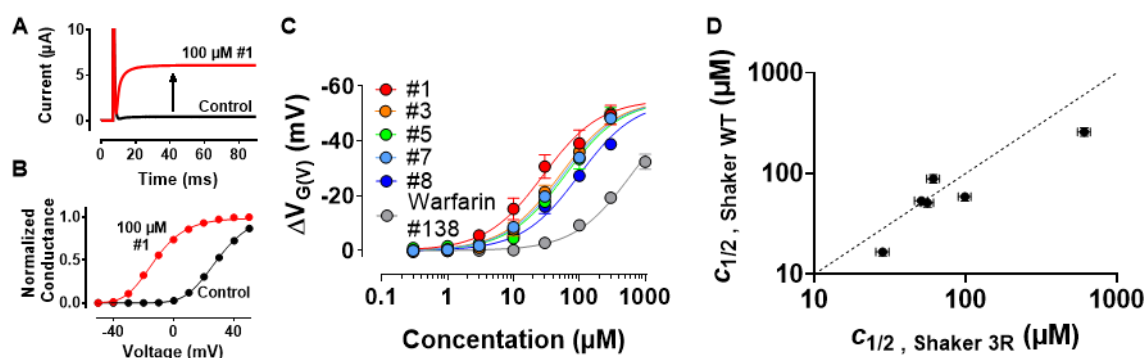
Fig. S4. **Effect of compounds #1, #3, #5, #7, #8, and warfarin (#138) on the 3R Shaker K$_V$ channel.** Expression in *Xenopus* oocytes, holding voltage = −80 mV, pH 7.4. Mean ± SEM, *n* is the number of experiments for each data point. (A) Effect of compound #1 on 3R Shaker K$_V$ channel at 0 mV. (B) *G*(*V*) curve for the cell in A. (C) Concentration-response curves for the 3R Shaker K$_V$ channel. V$_{MAX}$ = −55.1 ± 1.2 mV (shared for all compounds). $c_{1/2}$ (µM): 28.3 ± 2.8 (#1), 50.9 ± 5.0 (#3), 61.1 ± 6.0 (#5), 55.9 ± 5.4 (#7), 98.8 ± 9.5 (#8), 608 ± 59 (warfarin). *n* = 3-4. (D) Correlation curve for the compound affinity ($c_{1/2}$) on the WT versus 3R Shaker K$_V$ channel. Line show a 1:1 relationship. The affinities were not systematically affected.

11
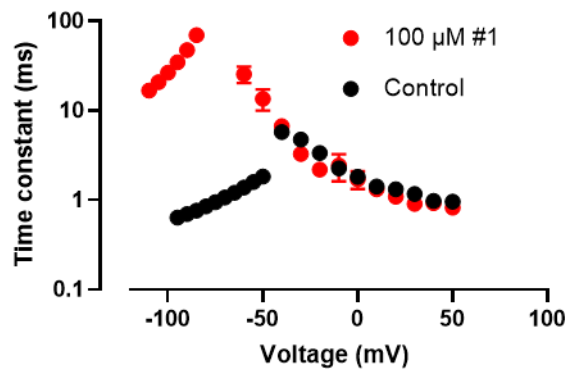
Fig. S5. Effects of compound #1 on the opening and closing kinetics of the WT Shaker K$_V$ channel. Black, control; Red, 100 μM compound #1, pH 7.4. Closing kinetics (−100 to −50 mV for control and −120 to −80 mV for compound #1) was measured in a high K$^+$ solution.
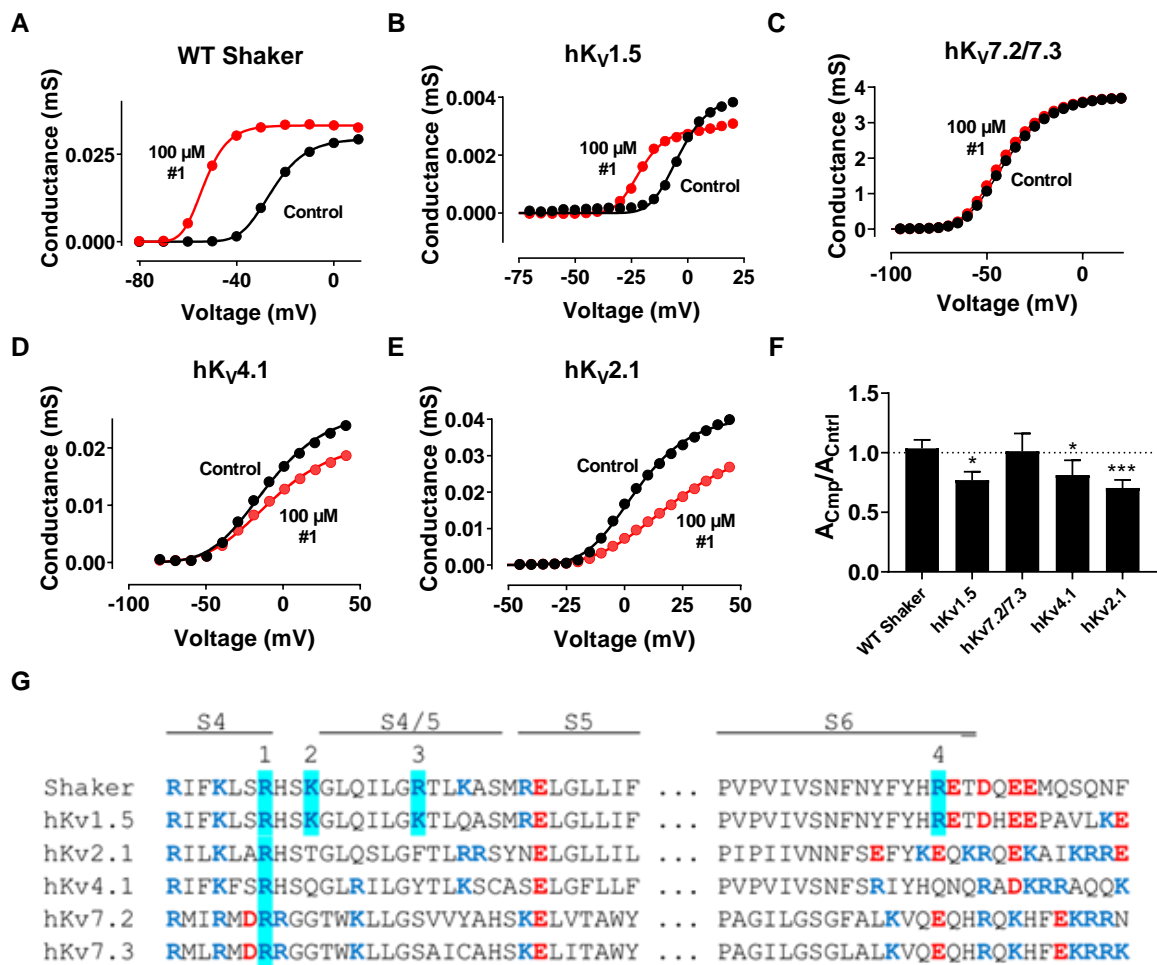
Fig. S6. **Effect of compound #1 on different K$_V$ channels**. (A-E) Expression system: *Xenopus* oocytes. pH = 7.4. *G(V)* curves before (black) and after application of 100 µM compound #1 (red), for indicated K$_V$ channels (see Fig. 4E for normalized *G(V)* curves). (F) Relative change in G$_{MAX}$ (= A$_{cmp}$/A$_{Cntrl}$) after application of 100 µM #1 for indicated K$_V$ channels. (G) To search for a possible binding-sites we compared the amino-acid sequences of all studied K$_V$ channels on the intracellular side in the vicinity on the transmembrane segments (up to 15 residues from the transmembrane segments). There are three positions where the residues are positively charged in K$_V$1.5 and Shaker K$_V$ and uncharged or negatively charged in the other channels. Two residues are located in the linker between S4 and S5 (K380 (=2) and R387 (=3) in the Shaker K$_V$ channel), which connects the voltage sensor to the pore gate. The third residue is located in intracellular end of S6 (R487 (=4) in the Shaker K$_V$ channel). 377 (=1) located in S4 is positively charged in all channels.

Fig. S7. Effects of compounds #1, #3, #5, #7, and #8 on Kv4.1. $c = 100 \, \mu M$, pH = 7.4. $n = 3$. (A) Effects on $G(V)$. (B) Effects on G_{MAX}.

A

Segment	Residue	1 (C)	2 (N)	3 (N)	5 (N)	9 (N)	11 (N)	12 (N)	14 (N)	10 (O)	4 (O)	6 (N)	7 (O)	8 (N)	13 (O)	16 (O)	Site A Mean	Site B Mean
N-S1	E218	0.00	0.24	0.00	0.44	0.00	0.00	0.16	0.00	0.00	0.02	0.40	0.02	0.08	0.00	0.00	0.11	0.09
N-S1	T219	0.00	0.18	0.00	0.36	0.00	0.00	0.16	0.00	0.00	0.06	0.05	0.02	0.08	0.00	0.00	0.09	0.04
S2-S3	R309	0.02	0.02	0.36	0.04	0.24	0.06	0.04	0.26	0.12	0.00	0.00	0.02	0.00	0.00	0.00	0.13	0.00
S2-S3	D310	0.02	0.30	0.72	0.36	0.58	0.92	0.38	0.62	0.38	0.14	0.21	0.14	0.08	0.00	0.20	0.49	0.13
S2-S3	V311	0.48	0.42	0.80	0.48	0.58	0.92	0.40	0.74	0.50	0.18	0.25	0.20	0.24	0.04	0.28	0.60	0.20
S2-S3	M312	0.42	0.32	0.80	0.42	0.32	0.90	0.06	0.04	0.44	0.14	0.07	0.16	0.12	0.02	0.26	0.41	0.13
S4-S5	F373	0.42	0.00	0.00	0.02	0.18	0.00	0.04	0.08	0.06	0.04	0.03	0.10	0.00	0.00	0.06	0.09	0.04
S4-S5	S376	0.22	0.02	0.04	0.08	0.04	0.00	0.00	0.00	0.04	0.10	0.00	0.06	0.00	0.00	0.10	0.05	0.04
S4-S5	R377	0.00	0.14	0.04	0.34	0.00	0.00	0.16	0.02	0.00	0.00	0.41	0.06	0.08	0.34	0.02	0.09	0.15
S4-S5	H378	0.00	0.16	0.00	0.12	0.00	0.02	0.36	0.10	0.26	0.16	0.32	0.12	0.08	0.36	0.38	0.10	0.24
S4-S5	S379	0.24	0.10	0.00	0.08	0.18	0.06	0.20	0.14	0.50	0.76	0.47	0.72	0.66	0.92	0.72	0.13	0.71
S4-S5	K380	0.26	0.30	0.00	0.40	0.18	0.12	0.24	0.14	0.50	0.76	0.61	0.74	0.70	0.94	0.72	0.21	0.75
S4-S5	G381	0.24	0.08	0.00	0.08	0.18	0.06	0.20	0.10	0.50	0.74	0.32	0.72	0.66	0.60	0.72	0.12	0.63
S4-S5	Q383	0.54	0.52	0.80	0.66	0.48	0.90	0.08	0.14	0.50	0.18	0.24	0.18	0.16	0.08	0.26	0.52	0.18
S4-S5	I384	0.14	0.20	0.08	0.34	0.00	0.90	0.00	0.00	0.00	0.00	0.20	0.02	0.04	0.02	0.00	0.21	0.05
S4-S5	G386	0.70	0.40	0.96	0.38	0.54	0.16	0.22	0.26	0.50	0.22	0.05	0.24	0.26	0.06	0.26	0.45	0.18
S4-S5	R387	0.48	0.42	0.80	0.46	0.58	0.88	0.44	0.64	0.50	0.16	0.21	0.18	0.20	0.04	0.28	0.59	0.18
S4-S5	T388	0.06	0.06	0.00	0.02	0.10	0.00	0.02	0.22	0.00	0.00	0.17	0.00	0.00	0.00	0.00	0.06	0.03
S4-S5	K390	0.28	0.10	0.28	0.08	0.42	0.04	0.12	0.28	0.08	0.06	0.21	0.06	0.06	0.02	0.06	0.20	0.08
S4-S5	A391	0.06	0.18	0.08	0.10	0.40	0.04	0.32	0.60	0.20	0.12	0.21	0.10	0.08	0.00	0.14	0.22	0.11
S4-S5	# R394	0.24	0.04	0.00	0.00	0.18	0.04	0.06	0.04	0.46	0.54	0.32	0.52	0.64	0.54	0.72	0.08	0.55
S4-S5	# G397	0.24	0.00	0.00	0.00	0.16	0.00	0.00	0.04	0.40	0.54	0.31	0.16	0.64	0.20	0.70	0.06	0.42
S4-S5	# L398	0.22	0.04	0.00	0.02	0.18	0.00	0.06	0.04	0.40	0.60	0.31	0.16	0.64	0.58	0.58	0.07	0.48
S6-C	F484	0.06	0.18	0.00	0.00	0.08	0.00	0.10	0.28	0.00	0.02	0.17	0.00	0.00	0.00	0.00	0.09	0.03
S6-C	R487	0.00	0.14	0.00	0.00	0.00	0.00	0.10	0.02	0.00	0.00	0.00	0.00	0.00	0.00	0.00	0.03	0.00
S6-C	E488	0.00	0.32	0.00	0.32	0.00	0.10	0.10	0.06	0.00	0.00	0.35	0.02	0.04	0.36	0.00	0.11	0.13
S6-C	A489	0.24	0.04	0.00	0.08	0.16	0.00	0.14	0.10	0.28	0.40	0.28	0.52	0.64	0.22	0.54	0.10	0.43

Column groupings: columns 1–14 = Site A compounds; column 10 = Site A/B; columns 4–16 = Site B compounds.

B

#3   #5   #8

R387   R387   K380   R394

Fig. S8. **The 15 most potent tautomer compounds docked against a tetrameric WT Shaker K$_V$ channel.** (A) Mean of average occupancy to residues in the tetrameric WT Shaker K$_V$ channel (see Supplementary Material and Methods). Positively charged residues are marked in blue, and negatively charged in red. The compounds could be grouped as Site-A compounds (interacting with residues 310-312, 383, 386, 387), or as Site-B compounds (interacting with residues 379-381, 394, 397, 398), except #10 (Table S1) that occupied both sites. (B) Best binding poses of compounds #3, #5, and #8. Compounds #3 and #5 prefer binding pose/site A (red). Compound #8 prefer binding pose/site B (blue).
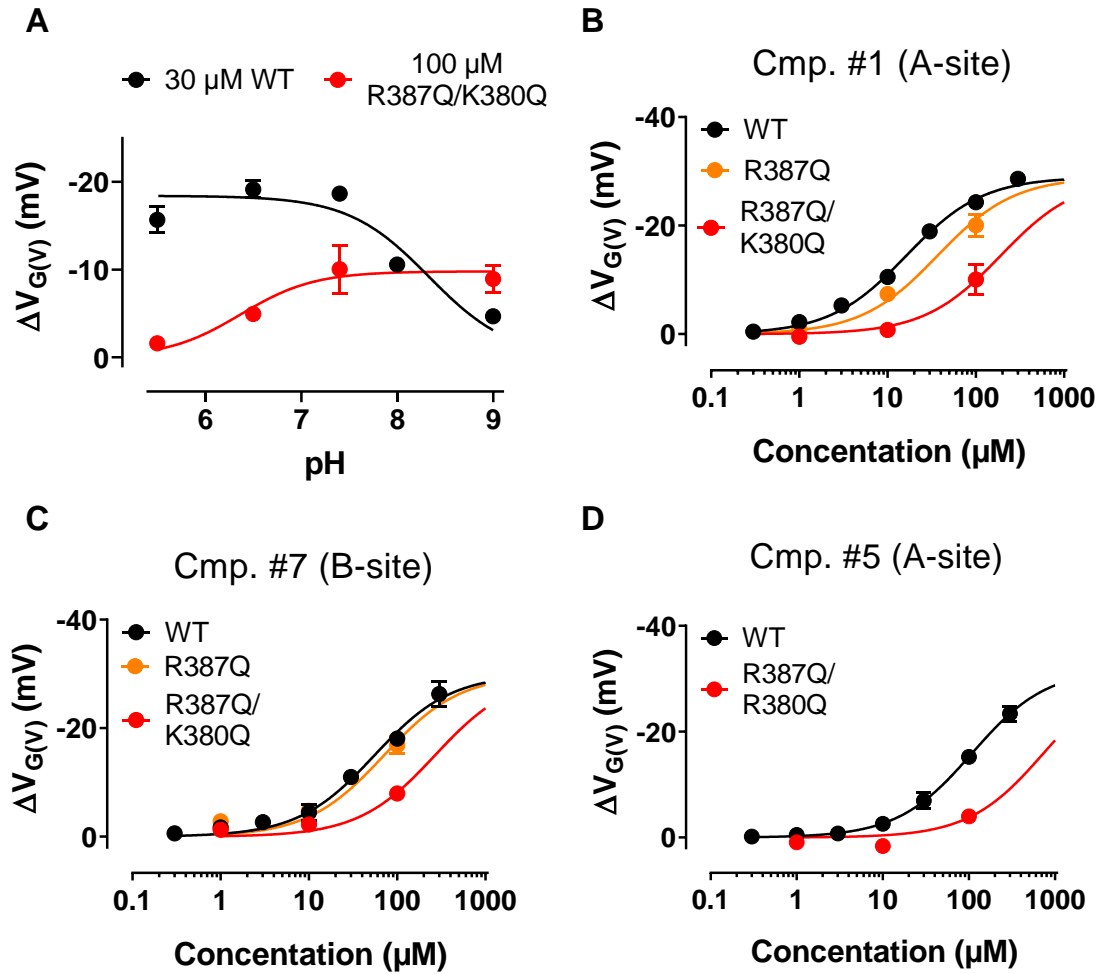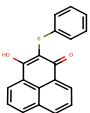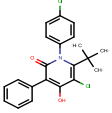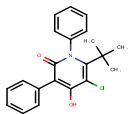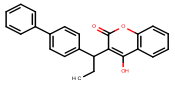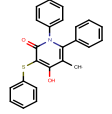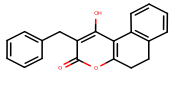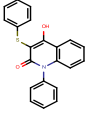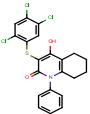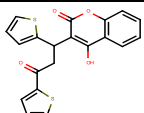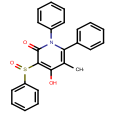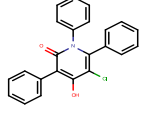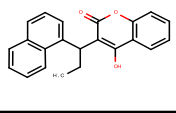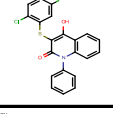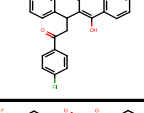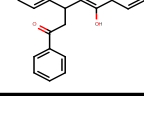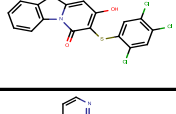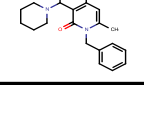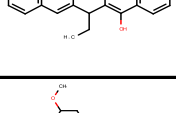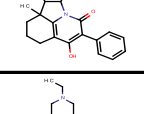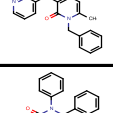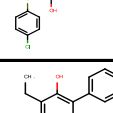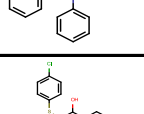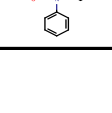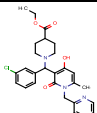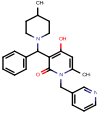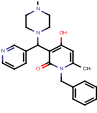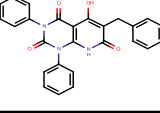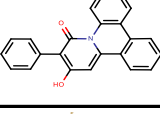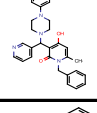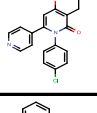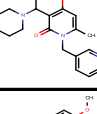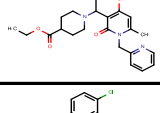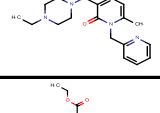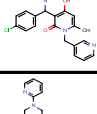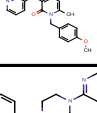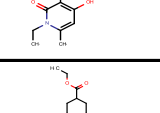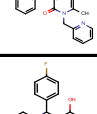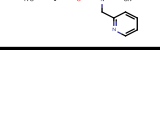
Fig. S9. Site A and Site B compounds effect on Shaker K$_V$ channel mutants. (A) pH dependence for *G(V)* shifts for 30 µM of compound #1 on WT Shaker (as in Fig. 3D; pK_a / ΔV_{MAX} WT: 8.3 / −18.1 (mV)) and 100 µM #1 on the R380K/R387Q mutant, pK_a / ΔV_{MAX}: 6.4 / −9.8 (mV). (B-D) Concentration-response curves for compound #1, #7, and #5 as denoted. All data mean ± SEM. *n* = 3-4. pH = 7.4. (B) $c_{½}$ (WT) = 16.3 ± 2.4 µM, $c_{½}$ (R387Q) = 36.9 ± 7.1 µM, $c_{½}$ (R380Q/R387Q) = 191.2 ± 32.6 µM, ΔV_{MAX} (shared value) = −29.0 ± 1.1 mV. (C) $c_{½}$ (WT) = 55.2 ± 11.7 µM, $c_{½}$ (R387Q) = 70.8 ± 15.7 µM, $c_{½}$ (R380Q/R387Q) = 267.6 ± 55.5 µM, ΔV_{MAX} (shared value) = −30.0 ± 2.1 mV. (D) $c_{½}$ (WT) = 108.9 ± 21.1 µM, $c_{½}$ (R387Q) = 736.9 ± 182.9 µM, ΔV_{MAX} (shared value) = −31.9 mV ± 2.5 mV.
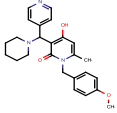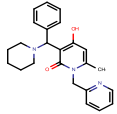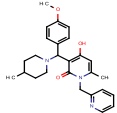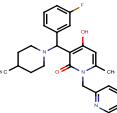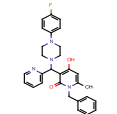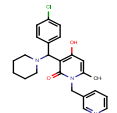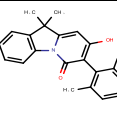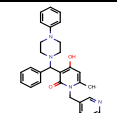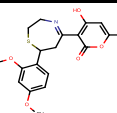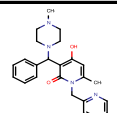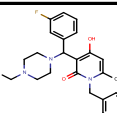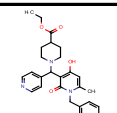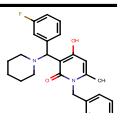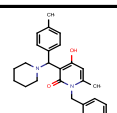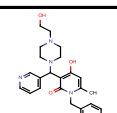
Table S1. Summary of high-throughput data, chemical data of the tautomer compounds and analysis data. *Cmp. Nr:* The compound number (effective order) used in the present investigation. *Structures:* Molecular structure of the compounds. *Type:* Denote the atom type in the central ring connected to side chain R2 (see Fig. 1C). *Exp:* Denotes experimental data, that is the effect on the current at +10 mV. 1.00 means no effect. Bold figures mean that the effect is statistically significantly different from 1 (see methods for calculation). n: Number of experiments carried out in the screen. *MW:* Molecular weight. *Log P:* Partition coefficient. *pKa:* Acid dissociation constant on a logarithmic scale. *R1-R4:* Denotes the calculated effect for the particular side chain in the molecule. The values can be compared with each other for a specific side chain but not between two different side chains. The value "1" is fixed for the most abundant side chains for R2, R3, and R4. "(1)" means that this is part of a ring structure. All effect is put in the column just before (1). The grey areas denote figures derived after the primary calculations, either because this side chain already was assigned a value from other compounds (R2 in #230, R2 in the O-compounds, R4 in #158) or if this is a unique side chain, that could be calculated afterwards. ND means that it was not possible to determine the value for this side chain. *Model:* Total predicted effect based on the side-chain analysis = R1 * R2 * R3 * R4. *Supplier ID:* Compound name used in the screen for identification
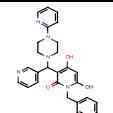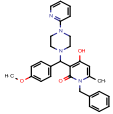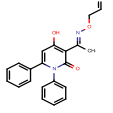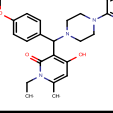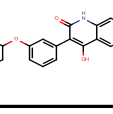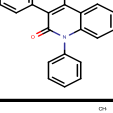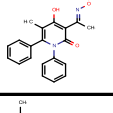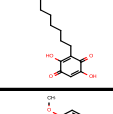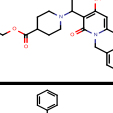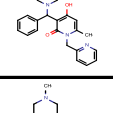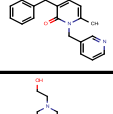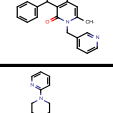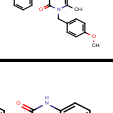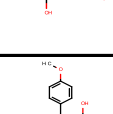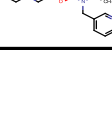
Cmp.Nr	Structure	Type	Exp	n	MW	LogP	pKa	R1	R2	R3	R4	Model	Supplier ID
1		C	**7.32**	2	304.4	3.91	6.02	8.73	0.84	(1)	(1)	7.32	AE-406/41056461
2		N	**7.19**	2	388.3	5.75	7.07	2.41	1.21	0.43	5.74	7.20	AE-406/41057002
3		N	**6.33**	2	353.9	5.14	7.43	2.41	1	0.43	5.74	5.95	AE-406/41056740
4		O	**6.19**	1	356.4	5.38	5.75	10.93	1.03	0.55	(1)	6.19	CBK016682
5		N	**6.18**	2	357.8	4.91	7.03	2.41	0.91	0.49	5.74	6.18	AE-406/41056741
6		N	**5.77**	1	385.5	5.07	7.66	8.73	1	0.35	1.85	5.65	RJC03393
7		O	**5.73**	2	304.3	4.17	7.47	2.08	1.03	2.67	(1)	5.73	AE-406/41056253
8		N	**4.62**	2	345.4	4.40	6.78	8.73	1	0.55	(1)	4.80	AE-406/41056299
9		N	**4.57**	2	452.8	6.29	6.81	5.92	1	0.73	(1)	4.32	AE-406/41057019

No.	Structure												ID
10		O	**4.55**	2	382.5	4.00	5.17	8.03	1.03	0.55	(1)	4.55	AO-476/43407292
11		N	**4.46**	2	401.5	3.95	6.92	6.88	1	0.35	1.85	4.46	AE-406/41056192
12		N	**4.19**	2	373.8	4.97	7.21	2.41	1	0.35	5.74	4.84	BTB11805
13		O	**4.11**	1	330.4	4.72	5.80	7.26	1.03	0.55	(1)	4.11	CBK016684
14		N	**4.00**	2	448.7	6.21	5.83	5.92	1	0.55	(1)	3.26	AE-406/41057021
15		O	**3.85**	2	434.9	4.62	5.11	6.79	1.03	0.55	(1)	3.85	AO-476/43407294
16		O	**3.83**	2	388.4	4.31	5.18	6.75	1.03	0.55	(1)	3.83	AO-476/43407293
17		N	**3.11**	2	438.8	5.97	6.85	5.92	0.53	(1)	1	3.14	AE-406/41056375
18		N	**3.04**	1	389.5	3.01	10.15	3.50	0.87	1	1	3.04	G747-0072
19		O	**2.87**	1	330.4	4.72	5.80	5.07	1.03	0.55	(1)	2.87	CBK016681
20		N	**2.69**	1	359.4	3.86	8.30	2.41	1.12	(1)	(1)	2.69	AE-406/41056421
21		N	**2.37**	1	418.5	2.36	10.17	2.33	0.87	1	1	2.03	G747-0076
22		N	**2.19**	1	405.9	5.43	7.41	3.35	1	0.35	1	1.17	AE-406/41056530
23		N	**2.16**	1	367.4	5.15	8.40	2.41	1	0.35	2.10	1.77	BTB11803
24		N	**2.08**	2	383.9	5.08	7.43	3.35	1	0.73	(1)	2.45	AE-406/41056894

25		N	**2.08**	1	412.6	5.38	7.91	5.94	1	0.35	1	2.08	AE-406/41057035
26		N	**2.04**	1	436.5	2.59	9.85	2.45	0.70	1	1	1.72	G747-0406
27		N	**2.04**	1	389.5	3.24	10.14	2.34	0.87	1	1	2.04	G747-0062
28		O	**1.89**	2	304.7	3.67	4.85	3.35	1.03	0.55	(1)	1.89	AE-406/41056931
29		N	**1.88**	2	379.9	5.00	6.42	3.35	1	0.55	(1)	1.84	AE-406/41056932
30		N	**1.85**	1	496.0	3.34	9.64	2.47	0.72	1	1	1.78	G747-0469
31		N	**1.84**	1	388.5	4.80	7.56	2.08	1.20	0.35	2.10	1.84	NRB04797
32		N	**1.75**	1	432.6	2.96	10.22	2.50	0.70	1	1	1.75	G747-0416
33		N	**1.74**	1	317.4	4.12	8.57	2.41	1	0.73	(1)	1.76	AE-406/41057102
34		N	**1.74**	1	423.9	3.61	9.81	2.42	0.72	1	1	1.74	G747-0468
35		N	**1.73**	1	461.6	2.73	9.94	1.99	0.87	1	1	1.73	G747-0073
36		N	**1.73**	1	453.0	2.97	9.84	2.40	0.72	1	1	1.73	G747-0475
37		N	**1.72**	1	484.6	4.04	9.79	2.01	0.72	1	1	1.45	G747-0485
38		N	**1.71**	1	379.9	4.98	7.84	2.41	1.21	0.54	1	1.57	AE-406/41056632
39		N	**1.67**	1	407.5	3.11	9.82	2.39	0.70	1	1	1.67	G747-0408

40		N	**1.66**	1	496.0	3.42	9.64	2.47	0.70	1	1	1.73	G747-0393
41		N	**1.66**	1	403.5	3.00	10.26	2.05	0.72	1	1	1.48	G747-0441
42		N	**1.66**	1	404.5	2.01	10.14	1.91	0.87	1	1	1.66	G747-0075
43		N	**1.65**	2	437.5	3.99	7.57	2.08	1	0.79	(1)	1.65	AE-406/41056103
44		N	**1.63**	1	337.4	4.14	8.54	2.41	0.68	(1)	1	1.63	AE-406/41056181
45		N	**1.62**	1	484.6	4.04	10.00	1.87	0.87	1	1	1.62	G747-0080
46		N	**1.62**	1	388.9	4.16	7.58	2.08	1.21	0.54	1	1.36	AE-406/41056370
47		N	**1.61**	1	389.5	2.78	10.20	2.21	0.72	1	1	1.59	G747-0439
48		N	**1.60**	1	491.6	2.66	9.85	2.09	0.70	1	1	1.46	G747-0380
49		N	**1.60**	1	453.0	3.05	9.84	1.96	0.70	1	1	1.37	G747-0394
50		N	**1.59**	1	496.0	3.34	9.64	2.20	0.72	1	1	1.59	G747-0473
51		N	**1.56**	1	497.6	3.12	9.77	1.75	0.84	1	1	1.47	G747-0159
52		N	**1.55**	1	404.5	3.12	10.11	1.75	0.64	1	1	1.12	G747-0183
53		N	**1.55**	1	479.6	2.96	9.65	2.21	0.70	1	1	1.55	G747-0404
54		N	**1.54**	1	421.5	3.38	9.87	2.20	0.70	1	1	1.54	G747-0410
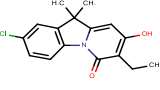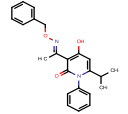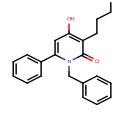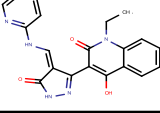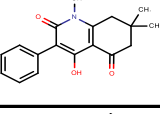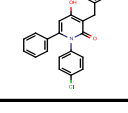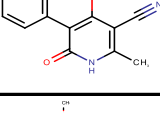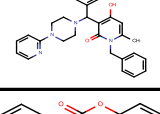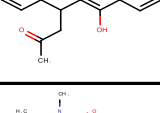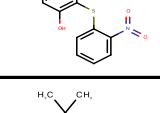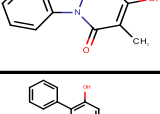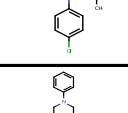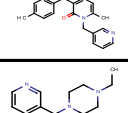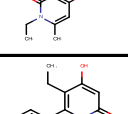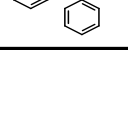
55		N	**1.53**	1	419.5	2.85	9.97	1.61	0.84	1	1	1.35	G747-0160
56		N	**1.53**	1	389.5	2.87	10.20	2.21	0.70	1	1	1.55	G747-0364
57		N	**1.52**	1	433.6	3.04	10.10	2.18	0.70	1	1	1.52	G747-0376
58		N	**1.50**	1	421.5	3.38	9.87	2.15	0.70	1	1	1.50	G747-0405
59		N	**1.50**	1	484.6	4.27	9.99	1.73	0.87	1	1	1.50	G747-0070
60		N	**1.48**	1	423.9	3.61	9.80	2.06	0.72	1	1	1.48	G747-0472
61		N	**1.47**	1	379.9	5.94	8.43	2.67	0.55	(1)	1	1.47	AE-406/41056822
62		N	**1.46**	1	466.6	3.90	10.09	1.99	0.72	1	1	1.43	G747-0444
63		O	**1.46**	1	375.4	2.69	7.20	1.42	1.03	1	1	1.46	KF 38789
64		N	**1.46**	1	404.5	2.09	10.15	1.99	0.70	1	1	1.39	G747-0367
65		N	**1.44**	1	436.5	2.50	9.85	2.45	0.72	1	1	1.76	G747-0484
66		N	**1.44**	1	461.6	2.73	9.94	1.65	0.87	1	1	1.44	G747-0083
67		N	**1.42**	1	407.5	3.03	9.82	1.85	0.72	1	1	1.33	G747-0481
68		N	**1.42**	1	403.5	3.31	10.24	1.86	0.72	1	1	1.34	G747-0491
69		N	**1.42**	1	434.5	1.32	10.08	1.63	0.87	1	1	1.42	G747-0078
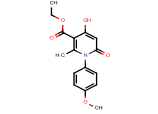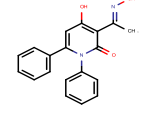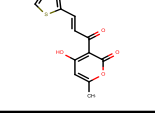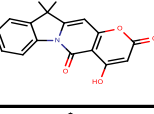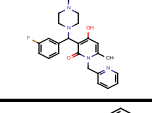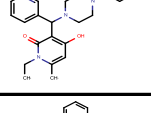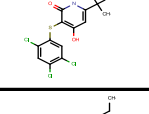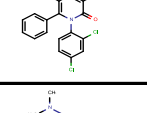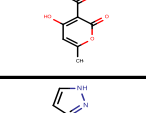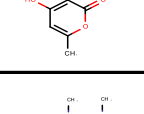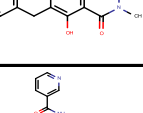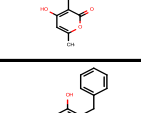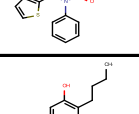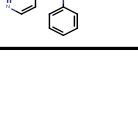
#	Structure												Name
70		N	**1.42**	1	467.6	3.27	9.92	1.75	0.87	1	1	1.52	G747-0081
71		N	**1.40**	1	496.6	4.33	10.00	1.61	0.87	1	1	1.40	G747-0010
72		N	**1.40**	1	360.4	3.83	7.74	2.57	1	0.35	1	0.90	AE-406/41057094
73		N	**1.39**	1	448.6	3.32	9.94	2.18	0.64	1	1	1.39	G747-0248
74		N	**1.39**	1	363.8	4.62	6.95	ND	0.91	ND	(1)	ND	L-701,324
75		N	**1.39**	2	313.4	4.03	7.46	2.41	1	0.55	(1)	1.33	ST073166
76		N	**1.38**	1	374.4	4.08	7.63	2.57	1	0.35	1.85	1.66	AE-406/41057153
77		C	**1.37**	1	294.4	4.83	5.16	ND	ND	ND	ND	ND	Embelin
78		N	**1.37**	1	491.6	2.58	9.85	2.09	0.72	1	1	1.50	G747-0455
79		N	**1.37**	1	466.6	3.98	10.09	1.99	0.70	1	1	1.39	G747-0369
80		N	**1.36**	1	404.5	2.01	10.15	1.99	0.72	1	1	1.43	G747-0442
81		N	**1.36**	1	434.5	1.32	10.08	1.89	0.72	1	1	1.36	G747-0445
82		N	**1.34**	1	496.6	4.33	9.95	1.75	0.84	1	1	1.47	G747-0106
83		N	**1.34**	1	295.3	3.02	7.01	2.08	0.91	0.71	(1)	1.34	ST081332
84		N	**1.34**	1	448.6	2.20	10.06	1.86	0.72	1	1	1.34	G747-0452

#	Structure												Code
85		N	**1.33**	1	484.6	4.63	9.81	1.53	0.87	1	1	1.33	G747-0039
86		N	**1.32**	1	496.0	3.42	9.64	1.89	0.70	1	1	1.32	G747-0390
87		N	**1.32**	1	419.5	2.71	10.05	1.84	0.72	1	1	1.32	G747-0449
88		N	**1.31**	1	466.6	4.49	10.11	1.75	0.87	1	1	1.52	G747-0005
89		N	**1.31**	1	434.5	2.12	10.05	1.77	0.61	1	1	1.08	G747-0359
90		N	**1.31**	1	345.4	4.70	8.64	2.41	1	0.54	(1)	1.31	AE-406/41056716
91		N	**1.31**	1	480.6	5.00	10.15	1.50	0.87	1	1	1.31	G747-0048
92		N	**1.31**	1	496.6	3.74	9.93	1.77	0.84	1	1	1.49	G747-0157
93		N	**1.30**	1	334.4	2.97	7.36	2.31	1	0.35	1.85	1.50	AE-406/41056099
94		N	**1.29**	1	433.6	3.02	10.01	1.50	0.84	1	1	1.26	G747-0162
95		N	**1.29**	1	303.4	3.80	8.62	2.41	0.53	(1)	1	1.28	NRB02860
96		O	**1.29**	1	331.3	2.49	5.69	1.68	1.03	0.75	(1)	1.29	NRB01625
97		N	**1.29**	1	461.6	2.82	9.95	1.84	0.70	1	1	1.29	G747-0365
98		N	**1.28**	1	467.6	3.27	9.92	1.75	0.72	1	1	1.26	G747-0448
99		N	**1.27**	1	403.5	3.30	10.19	1.50	0.87	1	1	1.31	G747-0084
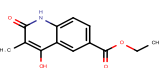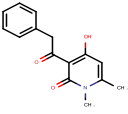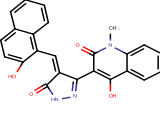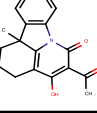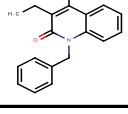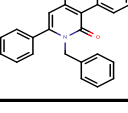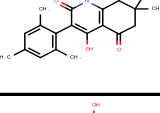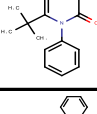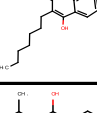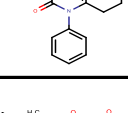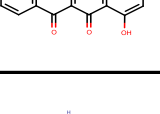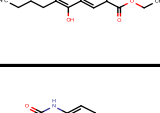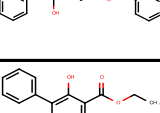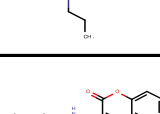
100		N	**1.27**	1	249.3	1.30	8.78	1.74	0.73	1	1	1.27	AE-406/41056161
101		N	**1.27**	1	343.4	3.83	7.57	2.08	1	0.61	1	1.27	AE-406/41056485
102		N	**1.27**	1	334.4	3.10	7.69	3.63	1	0.35	1	1.27	AE-406/41056442
103		N	**1.27**	1	484.6	4.04	9.81	1.46	0.87	1	1	1.27	G747-0079
104		N	**1.26**	1	407.5	3.23	9.81	1.80	0.70	1	1	1.26	G747-0398
105		N	**1.26**	1	497.6	3.35	9.75	1.50	0.84	1	1	1.26	G747-0151
106		N	**1.25**	1	484.6	4.12	9.80	1.79	0.70	1	1	1.25	G747-0412
107		N	**1.25**	1	283.4	3.11	7.89	2.22	1	0.54	1	1.20	AE-406/41056937
108		N	1.24	1	403.5	3.09	10.25	2.05	0.70	1	1	1.44	G747-0366
109		N	1.24	1	340.8	3.31	7.54	1.43	1.21	0.54	1	0.93	AE-406/41056379
110		N	1.24	1	461.6	2.97	9.93	1.42	0.87	1	1	1.24	G747-0063
111		N	1.24	1	386.5	0.59	10.14	2.33	0.61	1	1	1.42	G747-0358
112		N	1.23	1	496.6	3.74	9.99	1.71	0.72	1	1	1.23	G747-0453
113		N	1.23	1	484.6	4.12	10.01	1.75	0.70	1	1	1.23	G747-0372
114		N	1.22	1	403.5	3.40	10.24	1.86	0.70	1	1	1.30	G747-0413
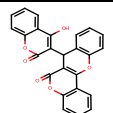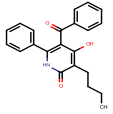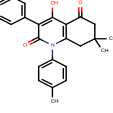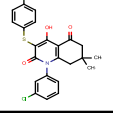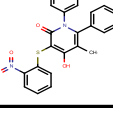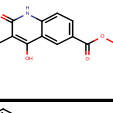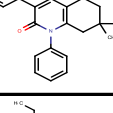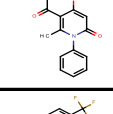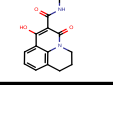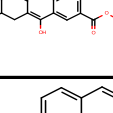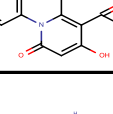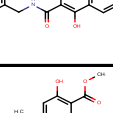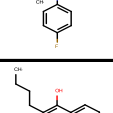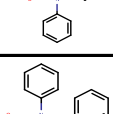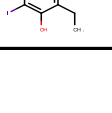
#	Structure												Code
115		N	1.22	1	328.4	3.63	8.02	2.08	1	0.43	1	0.89	AE-406/41056344
116		N	1.21	1	389.5	3.01	10.15	1.61	0.87	1	1	1.40	G747-0082
117		N	1.21	1	360.4	3.59	5.17	ND	0.91	ND	(1)	ND	A 769662
118		N	1.21	1	313.4	2.21	6.68	1.68	1.74	0.43	(1)	1.26	AE-406/41057105
119		N	1.21	1	496.6	3.97	9.91	1.43	0.84	1	1	1.21	G747-0149
120		N	1.20	1	407.5	3.12	9.82	1.85	0.70	1	1	1.30	G747-0403
121		N	1.20	1	484.6	4.27	9.80	1.38	0.87	1	1	1.20	G747-0069
122		N	1.20	1	263.7	2.14	4.92	ND	0.91	ND	(1)	ND	L-701,252
123		N	1.20	1	376.5	4.15	7.62	2.08	1	0.35	2.10	1.53	AE-406/41056352
124		N	1.20	1	409.5	5.31	9.05	2.67	0.91	0.35	1.42	1.21	AE-406/41057001
125		N	1.20	1	314.4	3.25	8.00	2.08	1	0.49	1	1.02	AE-406/41057152
126		N	1.20	1	484.6	4.04	9.81	1.69	0.72	1	1	1.22	G747-0446
127		N	1.20	1	484.6	4.12	9.81	1.69	0.70	1	1	1.18	G747-0371
128		N	1.20	1	467.6	3.35	9.92	1.75	0.70	1	1	1.23	G747-0373
129		N	1.19	1	453.0	2.97	9.84	1.96	0.72	1	1	1.41	G747-0471
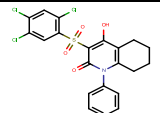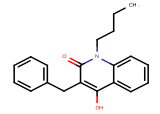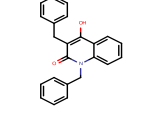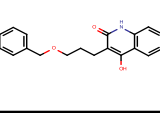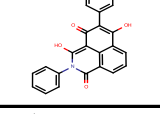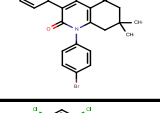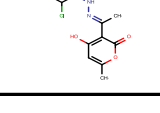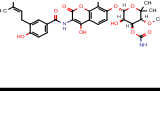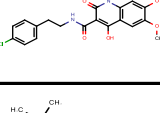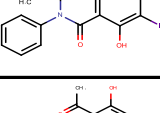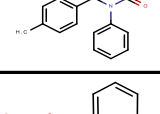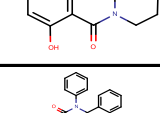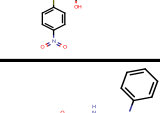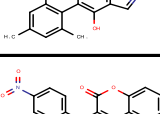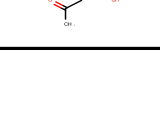
130		N	1.19	1	289.8	3.57	7.83	2.02	0.55	(1)	1	1.11	AE-406/41056654
131		N	1.19	1	376.5	4.62	7.95	2.43	1	0.49	1	1.19	AE-406/41056667
132		N	1.19	1	333.4	4.59	10.38	2.04	0.87	0.35	1	0.62	RJC03582
133		N	1.18	1	375.4	0.50	10.98	3.35	0.64	0.55	(1)	1.18	ST044367
134		N	1.18	1	297.4	2.38	9.18	2.41	0.73	0.43	(1)	0.76	AE-406/41056058
135		N	1.18	1	387.9	5.38	7.80	2.08	1.21	0.35	1	0.88	AE-406/41057207
136		N	1.18	1	226.2	1.15	11.36	2.41	0.91	1	0.56	1.23	RJC03342
137		N	1.18	1	496.6	4.33	10.00	1.36	0.87	1	1	1.18	G747-0015
138		O	**1.18**	7	308.3	2.74	5.56	2.08	1.03	0.55	(1)	1.18	SAM002554882
139		N	1.17	1	292.3	2.02	9.25	1.55	0.73	1	1	1.13	AE-406/41056303
140		N	1.17	1	241.3	2.52	8.35	2.22	0.53	(1)	1	1.18	AE-406/41057096
141		N	1.17	1	339.8	4.86	8.33	2.41	1.21	0.49	1	1.43	RJC03583
142		N	1.16	1	480.6	4.41	10.13	1.61	0.72	1	1	1.16	G747-0495
143		N	1.15	1	356.5	0.99	10.19	2.33	0.64	1	1	1.49	G747-0261
144		N	1.15	1	291.4	3.49	8.23	1.68	1	0.35	2.10	1.23	AE-406/41056342
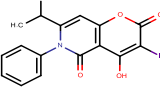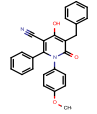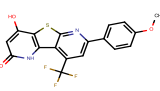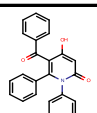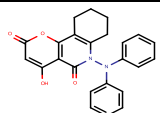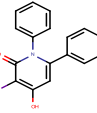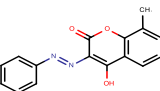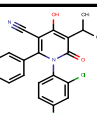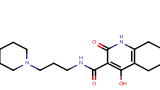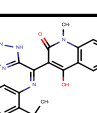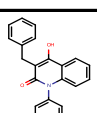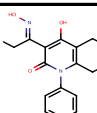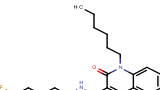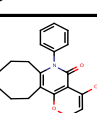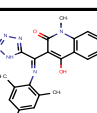
#	Structure											ID
145		N	1.15	1	275.7	3.13	7.79	2.22	0.55	(1)	1	1.22	AE-406/41057142
146		N	1.15	1	303.3	1.71	6.03	1.68	1.74	1	0.39	1.15	AB-321/43115463
147		N	1.15	1	320.3	2.72	7.42	2.31	1	0.35	1	0.81	RJC00801
148		O	1.14	1	262.3	2.74	6.50	1.11	1.03	1	1	1.14	AN-829/25042008
149		O	1.14	1	295.3	1.83	5.68	1.68	1.03	0.66	(1)	1.14	NRB05091
150		N	1.13	1	484.6	4.12	9.79	2.01	0.70	1	1	1.41	G747-0407
151		N	1.13	1	404.5	2.53	10.09	1.77	0.64	1	1	1.13	G747-0262
152		N	1.13	1	454.8	6.81	7.02	5.92	1	0.43	1	2.55	AE-406/41057203
153		N	1.13	1	413.3	5.39	5.89	2.04	2.81	0.35	0.56	1.12	AE-406/41057212
154		O	1.13	1	223.2	0.81	6.74	1.10	1.03	1	1	1.13	BTB10069
155		O	1.13	1	192.2	0.91	6.90	1.10	1.03	1	1	1.13	RF01179
156		N	1.13	1	327.3	0.89	8.29	2.08	0.73	0.74	(1)	1.13	JFD02468
157		O	1.12	1	287.3	0.53	6.83	1.09	1.03	1	1	1.12	AP-060/15175005
158		N	1.12	1	359.4	4.68	7.91	2.08	1	0.54	1	1.12	AE-406/41056563
159		N	1.12	1	320.4	3.31	8.03	2.04	1	0.54	1	1.10	AE-406/41056627
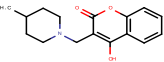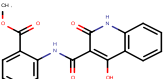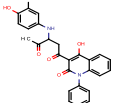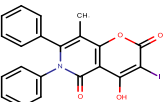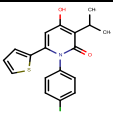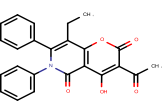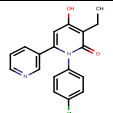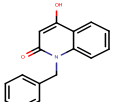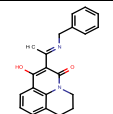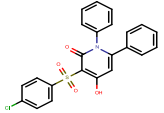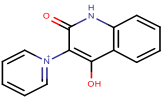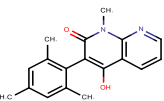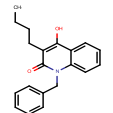
No.	Structure													ID
160		N	1.12	1	374.8	3.85	7.89	2.41	1.21	0.54	1		1.57	AE-406/41057038
161		O	1.11	1	243.2	0.41	5.46	1.68	1.03	0.64	(1)		1.11	BTB12394
162		O	1.10	1	345.4	2.89	5.59	2.22	1.03	0.48	(1)		1.10	AE-406/41057131
163		N	1.10	1	292.3	2.42	7.94	2.02	1	0.54	1		1.09	AE-406/41057221
164		N	1.10	1	271.3	2.51	7.38	1.84	1	0.49	1		0.90	AE-406/41057085
165		N	1.09	1	281.3	2.66	6.96	2.08	0.91	0.58	(1)		1.09	ST078022
166		N	1.09	1	319.4	2.96	6.99	1.84	1	0.35	1.85		1.19	AE-406/41057034
167		N	1.09	1	253.3	2.35	8.25	1.68	0.61	(1)	(1)		1.02	AE-406/41056760
168		N	1.09	1	368.6	2.64	6.49	1.19	0.91	1	1		1.08	AE-406/41056786
169		N	1.09	1	354.8	3.91	7.61	2.04	1.21	0.35	1		0.86	AE-406/41057213
170		O	1.09	1	264.7	2.01	5.46	1.68	1.03	ND	ND		ND	AB-321/43115441
171		O	1.08	1	323.3	2.59	5.79	1.68	1.03	0.62	(1)		1.08	AE-406/41056176
172		N	1.08	1	317.8	3.34	6.50	3.35	0.73	0.55	(1)		1.35	AE-406/41057009
173		N	1.08	1	317.8	2.97	6.50	1.68	1.21	0.43	(1)		0.87	AE-406/41057165
174		N	1.08	1	241.3	2.45	8.41	1.68	1	0.73	(1)		1.23	BTB11567

No.	Structure												Code
175		N	1.07	1	247.3	1.60	6.59	2.22	0.91	0.52	(1)	1.05	ST072283
176		N	1.07	1	257.3	1.79	9.39	1.47	0.73	1	1	1.07	AE-406/41056965
177		N	1.07	2	411.4	2.90	5.70	2.65	0.73	0.55	(1)	1.07	ST042085
178		N	1.06	1	295.3	2.27	7.02	1.84	0.61	(1)	(1)	1.12	AE-406/41056820
179		N	1.05	1	279.3	3.27	7.40	2.02	0.87	0.55	(1)	0.97	ST072291
180		N	1.05	1	353.4	4.53	10.55	2.41	0.87	0.35	1	0.73	AE-406/41057087
181		N	1.04	1	325.4	3.69	9.38	2.67	0.91	0.43	(1)	1.04	AE-406/41056995
182		N	1.04	1	243.3	2.97	8.68	1.68	1	0.43	1	0.72	AE-406/41057095
183		N	1.04	1	333.4	5.11	7.43	ND	ND	(1)	(1)	ND	BTB10330
184		N	1.03	1	283.4	3.58	8.32	1.43	1	0.73	(1)	1.04	AE-406/41056594
185		O	1.03	1	298.3	1.97	5.03	1.68	1.03	0.60	(1)	1.03	AB-321/43115514
186		N	1.02	1	289.3	2.93	6.77	2.04	0.91	0.52	(1)	0.97	ST073151
187		N	1.01	1	343.4	4.08	7.35	2.41	0.91	0.46	(1)	1.01	ST072285
188		N	1.01	1	315.4	2.76	8.62	2.41	1.07	1	0.39	1.01	AE-406/41056062
189		O	0.99	1	295.3	0.71	5.03	1.75	1.03	0.55	(1)	0.99	ST057506

190		O	0.98	1	410.4	3.19	5.12	1.73	1.03	0.55	(1)	0.98	ST051983
191		N	0.96	1	347.4	3.83	8.66	2.04	0.91	0.35	1.42	0.92	AE-406/41056508
192		N	0.96	1	373.5	4.55	7.23	2.41	1.21	0.43	(1)	1.25	AE-406/41056684
193		N	0.95	1	460.4	5.61	5.82	3.35	0.66	0.43	(1)	0.95	AE-406/41056544
194		N	0.95	2	430.5	5.01	7.15	1.55	1	0.35	1.85	1.00	AE-406/41056685
195		N	0.94	1	261.3	2.04	6.64	2.02	0.91	0.52	(1)	0.96	ST073152
196		N	0.94	1	359.4	4.04	7.18	2.41	1	0.43	(1)	1.04	AE-406/41056356
197		N	0.93	1	285.3	3.06	7.08	1.68	1	1	0.55	0.93	AB-321/43115518
198		N	0.92	1	388.3	3.09	5.35	ND	ND	(1)	(1)	ND	JFD03180
199		N	0.91	1	323.3	3.18	6.70	2.08	0.91	0.52	(1)	0.98	ST072290
200		N	0.90	1	355.4	3.55	6.91	1.68	1	ND	ND	ND	AB-321/43115442
201		N	0.89	1	355.4	-0.34	5.43	ND	0.91	ND	(1)	ND	ST073264
202		N	0.89	1	319.3	3.08	6.30	0.79	0.91	1.24	1	0.89	AE-406/41056309
203		N	0.88	1	293.4	4.09	7.22	2.04	1	0.55	(1)	1.12	ST073165
204		N	0.86	1	417.2	4.47	6.79	1.38	1	0.35	2.10	1.01	AE-406/41056443

	Structure												
205		N	0.86	1	484.8	5.27	4.71	1.19	1	0.73	(1)	0.87	AE-406/41056628
206		N	0.86	1	307.4	4.01	7.46	2.08	0.75	0.55	(1)	0.86	NRB02128
207		N	0.85	1	341.4	4.41	7.37	2.08	0.87	0.55	(1)	1.00	ST072292
208		N	0.85	1	309.4	3.06	7.29	1.70	0.91	0.55	(1)	0.85	AE-562/12222668
209		C	0.85	1	381.4	4.46	6.07	2.41	0.35	(1)	(1)	0.85	AE-406/41056537
210		N	0.85	1	438.3	4.80	6.76	2.41	0.82	0.43	(1)	0.85	AE-406/41056715
211		O	0.85	1	361.6	4.39	6.19	0.83	1.03	1	1	0.85	CD10299
212		O	0.85	2	612.6	3.26	5.51	ND	1.03	ND	(1)	ND	Prestw-834
213		N	0.84	1	402.8	2.15	5.34	ND	0.91	ND	(1)	ND	CBK159986
214		O	0.83	1	437.2	3.65	4.49	1.38	1.03	0.58	(1)	0.83	AE-406/41056184
215		N	0.82	1	319.4	3.08	6.84	1.68	1	ND	ND	ND	AB-321/43115440
216		O	0.81	1	269.3	0.89	5.49	1.68	1.03	0.47	(1)	0.81	BTB09370
217		N	0.80	1	416.5	4.77	7.28	2.29	1	0.35	1	0.80	AE-406/41056055
218		N	0.80	1	345.4	4.23	5.79	2.67	0.91	0.33	(1)	0.80	AE-406/41056994
219		O	0.79	1	353.3	2.68	5.02	1.39	1.03	0.55	(1)	0.79	Prestw-110

220		O	0.79	1	423.2	3.27	4.44	1.38	1.03	0.56	(1)	0.79	AE-406/41056097
221		N	0.78	1	408.5	4.27	6.30	2.08	1.74	0.35	0.56	0.71	AE-406/41056596
222		N	0.78	1	392.4	3.76	4.99	1.68	0.91	0.51	(1)	0.78	AM-807/14144078
223		N	0.78	1	367.4	3.99	6.70	1.68	1	0.35	1.42	0.83	AB-321/43115390
224		O	**0.78**	2	400.4	3.84	6.02	1.68	1.03	0.45	(1)	0.78	AB-321/43115528
225		N	**0.78**	2	389.2	3.78	6.86	1.38	1	0.35	1	0.48	AE-406/41056340
226		O	0.77	1	280.3	3.57	4.87	ND	1.03	ND	(1)	ND	JFD02617
227		N	**0.77**	2	399.3	4.79	5.80	1.43	2.81	0.35	0.56	0.79	AE-406/41057211
228		N	0.76	1	333.4	0.28	10.41	1.14	0.91	0.73	(1)	0.76	ST073380
229		N	0.76	1	402.5	3.39	5.66	1.89	0.73	0.55	(1)	0.76	AE-406/41056428
230		N	0.75	1	327.4	4.34	7.12	2.08	1	0.55	(1)	1.14	ST072306
231		N	**0.74**	2	312.4	3.08	10.63	1.01	1	0.73	(1)	0.74	AE-406/41056168
232		N	**0.73**	1	409.5	3.98	5.20	ND	ND	0.55	(1)	ND	AG-690/11231116
233		O	**0.73**	1	337.4	3.03	5.83	1.68	1.03	0.42	(1)	0.73	AE-406/41056177
234		N	**0.70**	1	388.4	3.38	5.66	1.74	0.73	0.55	(1)	0.70	AE-406/41056491

No.	Structure	Atom	Val		M.W.	cLogP	pKa	A	B	C	(D)	E	ID
235		O	**0.69**	1	273.3	-0.02	4.86	1.22	1.03	0.55	(1)	0.69	ST038449
236		N	**0.69**	1	338.3	2.52	5.73	1.38	0.91	0.55	(1)	0.69	ST079103
237		N	**0.67**	1	456.5	3.68	5.48	1.22	1	0.55	(1)	0.67	ST023441
238		O	**0.67**	1	471.3	3.72	4.40	1.38	1.03	0.47	(1)	0.67	AE-406/41056441
239		N	**0.66**	1	345.8	4.44	7.50	1.43	1.21	0.54	1	0.93	AE-406/41056573
240		O	**0.65**	1	401.4	3.10	4.69	1.84	1.03	0.34	(1)	0.65	AE-406/41056360
241		N	**0.65**	1	326.8	3.02	7.49	2.02	1.21	0.35	1	0.86	AE-406/41056590
242		N	**0.63**	1	251.3	2.43	7.46	1.68	0.87	0.55	(1)	0.80	ST057318
243		N	**0.63**	1	332.4	3.07	6.04	ND	ND	(1)	(1)	ND	AE-406/41056175
244		N	**0.63**	1	437.9	4.41	5.23	1.80	1	0.35	1	0.63	AE-406/41056362
245		N	**0.62**	1	239.3	-2.60	2.86	1.24	0.91	0.55	(1)	0.62	ST071870
246		N	**0.58**	1	294.4	3.29	6.96	2.67	0.73	0.30	(1)	0.58	AE-406/41057000
247		N	**0.56**	1	307.4	4.16	7.48	2.04	0.87	0.55	(1)	0.98	ST073153